J. Plasma Fusion Res. SERIES, Vol. 2 (1999) 153–156

Two-Dimensional Simulations of Relativistic Jet-Cloud Collisions

ZHANG Hui-Min, KOIDE Shinji and SAKAI Jun-Ichi
Faculty of Engineering, Toyama University, 3190 Gofuku, Toyama 930-8555, Japan

(Received: 8 December 1998 / Accepted: 20 May 1999)

Abstract

We present two-dimensional simulation results of jet-cloud collision, by using a relativistic hydrodynamic simulation code. It is shown that the collision processes are rather different for relativistic and nonrelativistic jet. For the relativistic jet, the collision takes the form of reflection. The deflection angle can be greater than 90°. The jet material is heated and suffers rapid deceleration and reacceleration in collision region. While a nonrelativistic jet is smoothly bent to a small angle 80°, the pressure and temperature is only a little higher than their initial values. These results are useful for understanding some observations.

Keywords:
galaxies, jets, hydrodynamics, jet-cloud collision

1. Introduction

Observational studies of jet in extragalactic radio sources show that the jets are often bent through large apparent angles [1-5]. The bending could result from a variety of mechanisms. However, some jet apparently changes direction at the location of the bright region and optical knot [6]; some jets are bent by deflection angle greater than 90° [7]. It seems that without using a jet-cloud collision model it is impossible to explain them. Some observations have also presented compelling evidence for the relativistic flow in most of jets [1-4,8,9]. Thus, relativistic simulation should also be used to investigate jet concerned processes [10-19]. Here, we report our simulation results of jet-cloud collision by using a special relativistic hydrodynamic (RHD) code in which a simplified total variation diminishing (TVD) method was employed.

2. Initial Condition and Results

We carried out two simulations for relativistic R and nonrelativistic N case, respectively. In our simulations, the length, density and pressure are normalized by a, ρ_0 and p_0, respectively. The system sizes are $0 \le x \le 25a$ and $-11a \le y \le 14a$ in the x and y directions The number of mesh points are 190×190. Initially, the jet, ambient medium and cloud start with equal pressure p_0, and adiabatic index is $\Gamma = 5/3$. The density of ambient medium, jet and cloud are $1.0\rho_0$, $0.1\rho_0$, and $1000.0\rho_0$, respectively. The jet and cloud radii a and $5a$. The jet is injected from the orifice at the left boundary of the calculation box; $x/a = 0$, $-1 \le y/a \le 1$. The left surface $x = 0$ is bounded by the fixed condition. We use a simplified radiative boundary condition at $x = 25a$ and $y = -11a$ and $y = 14a$. Along the z-direction for the slab geometry, we use the periodic boundary condition. Initially, the cloud center is localed at $x/a = 15$, $y/a = -2.5$. The impact parameter of collision is $2.5a$ for two runs. The velocities are normalized by sound speeds $v_s^N \equiv \sqrt{(\Gamma p/\rho_a)} = 1$, $v_s^R \equiv \sqrt{\Gamma p/(\rho_a + p/(\Gamma - 1)c^2)} = 1$ for nonrelativistic and relativistic cases, respectively. Time units are $\tau_s^N =$

Corresponding author's e-mail(HMZ): zhanghm@ecs.toyama-u.ac.jp

a/v_s^N and $\tau_s^R = a/v_s^R$. The injection velocities are of Mach number 4.0, and Lorentz factor 4.56 and 1.005 for relativistic and nonrelativistic jet, respectively.

Figure 1 shows the distribution of main physical quantities of R at the time $t = 44.9\tau_s^R$. As seen in Figure 1 the jet hits the cloud and a high pressure region is formed, where the maximum pressure is as high as $22.7p_0$. This region is bound on the one side by the

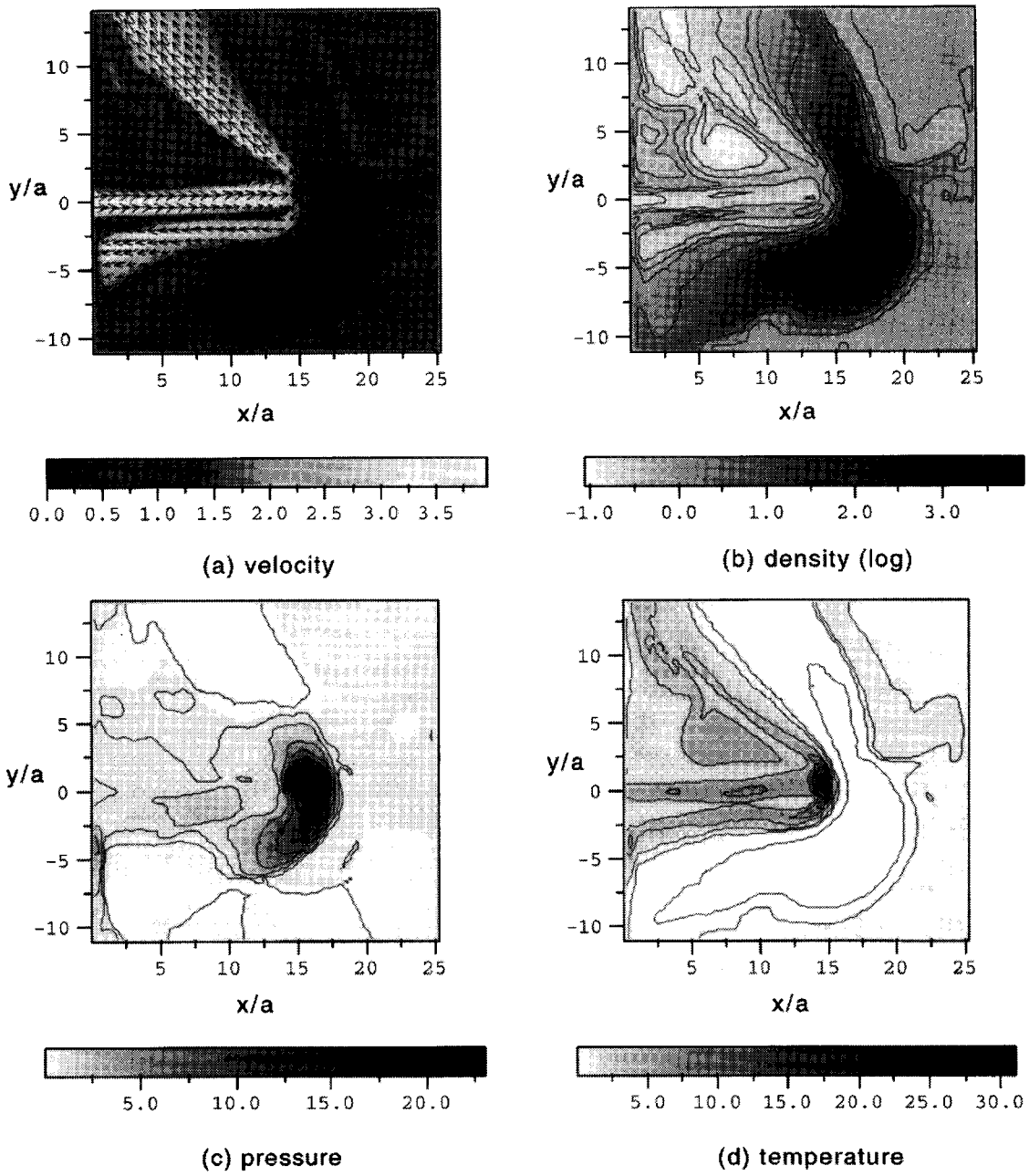

Fig. 1 **(a)** Velocity distribution of R at $t = 44.9\tau_s^N$. The jet rushes at the cloud and forms two downstream flows, the deflection angle of the dominant flow is about 130°. The original jet decelerates by a shock, and then the gas is reaccelerated to supersonic speed. **(b)** Density distribution. The cloud sharp is changed. A bow shock drives into the cloud. **(c)** Pressure distribution. The high pressure region is bound by two shocks, the one is at the beam head, the other one is a transform of bow shock driven into the cloud. **(d)** Temperature distribution. The temperature in the collision region is high.

shock driven into the cloud and on the other side by a shock at the head of jet beam. The contact discontinuity is located in the high pressure region. The left half of the high pressure region is filled with thermalized jet material; the other half is high density and pressure cloud gas. The maximum value of temperature $T(= p/\rho)$ in the collision region is about 30 times of the initial ambient temperature, or, the jet gas is heated to about 6 times of its injection temperature. The two tips of the region are just two nozzles from which the high pressure

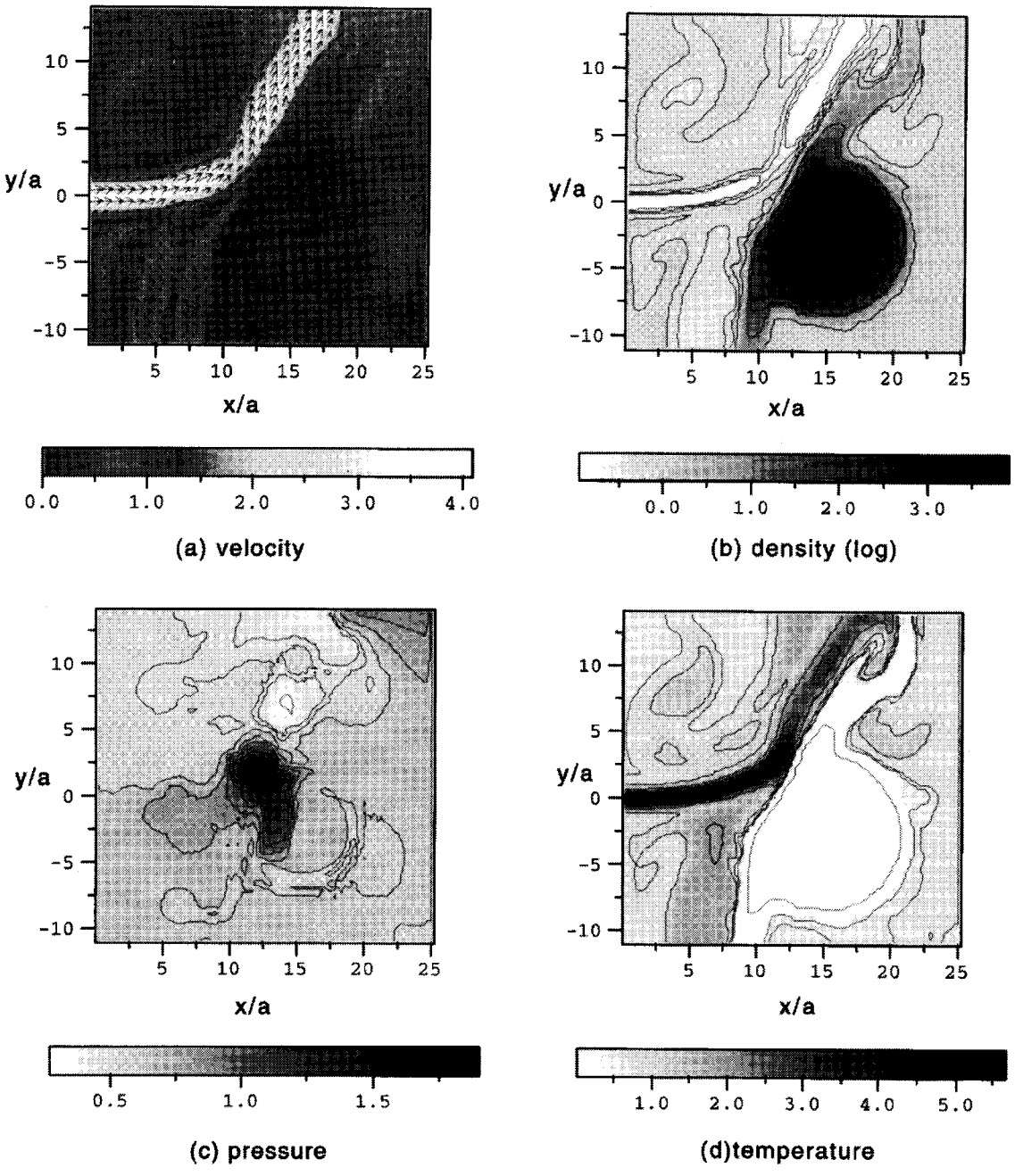

Fig. 2 **(a)** Velocity distribution of N at $t = 83.5\tau_s^N$. The jet is gradually bent to about 60° by the cloud. When it touch the cloud, its velocity is decelerated but is still supersonic. **(b)** Density distribution. The sharp of the cloud is changed. **(c)** Pressure distribution. **(d)** Temperature distribution. The temperature in the collision region is almost the same as the that of injection jet.

gas spurts out and forms two supersonic downstream flows. The one located on the upside is dominant, it inherits most of the original jet material and energy. The downstream flow is supersonic and of low density, the deflection angle is about 130° with an opening angle. During the collision, the jet gas suffers rapid deceleration and reacceleration. The region which takes decisive effect on the advance direction of downstream flows is just the small high pressure region.

Figure 2 Shows the distribution of main physical quantities of N at the time $t = 83.5\tau_s^N$. The jet is bent and finally rushes out from the calculation box with the deflection angle 80°. Almost all of the original jet material inherited by this downstream flow, there is nearly no secondary downstream flow. The contact discontinuity is almost a straight line. No clear deceleration and reacceleration appears. However the pressure and temperature at the impact point is higher, the maximum pressure is about 1.8 times of their initial values. The gas temperature in the collision region is almost the same as the injection jet temperature. In fact, as time goes, the cloud shape gradually changes, and around the cloud, the density and pressure are no longer uniform, they are higher than those of ambient medium. As seen in the Figure 2, the jet deflection is a gradual process. First, due to the back-flow of the secondary downstream, the jet begins to change its direction early, then it is bent by the cloud, finally the higher pressure and density around the cloud cause further deflection. During this process, jet does not suffer rapid deceleration and reacceleration.

3. Conclusions

Two-dimensional simulations show that relativistic jet-cloud collision takes the form of reflection and the deflection angle can greater than 90°. A reflection process is usually accompanied with violent physical processes, rapid deceleration and reacceleration, high pressure and temperature in the collision region. While a nonrelativistic jet is smoothly bent to a small angle, the pressure and temperature is only a little higher than their initial values. These results are useful for understanding some observations such as the wide-angle tailed radio galaxy 1919+479 and the BL lac object 3C 371.

Acknoweldgment

Sakai thanks the Cosel company for the support. Zhang is grateful to the Japanese Education Ministry for a scholarship.

References

[1] R. Fejes, R.W. Porcas and C.E. Akujar, Astron. Astrophys. **257**, 459 (1992).

[2] C. Hummel, T. Muxlow, T. Krichbaum, A. Quirrenbach, C. Schalinski, A. Witzed and K.J. Johnston, Astron. Astrophys. **262**, 295 (1992).

[3] K.E. Conway and R. Davis, Astrophys. J **345**, L21 (1994).

[4] T.U. Cawthorne, in *Beams and Jets in Astrophysics*, ed. P.A. Hughes (Combridge: Cambridge Univ. Press), 187 (1991).

[5] R.L. Mutel, in *Proc, Parsec-Scale Radio Jet Workshop*, ed J.A. Zensus & K.I. Kellerman (Green Bank: NRAO), 191 (1989).

[6] K. Nilsson, J. Heidt, T. Pursimo, A. Sillanpää, L.O. Takalo and K. Jäger, Astrophys. J. **484**, L107 (1997).

[7] J.O. Burns, C.P. O'Dea, S.A. Gregory and T.J. Balonek, ApJ **307**, 73 (1986).

[8] K.E. Conway and R. Davis, Astrophys. J. **345**, L21 (1994).

[9] D.C. Gabuzda, J.F.C. Wardle and D.H. Roberts, Astrophys. J. **336**, L59 (1989).

[10] R.T. Emmering and R.A. Chevalier, Astrophys. J. **321**, 334 (1994).

[11] E. Corbelli and P. Veltri, Astrophys. J. **340**, 679 (1989).

[12] F.V. Coroniti, Astrophys. J. **349**, 538 (1990).

[13] Y.-Q. Lou, Astrophys. J. **397**, L67 (1992).

[14] Y.-Q. Lou, Monthly Notices Royal Astron. Soc. **279**, 129.

[15] S.V. Bogovalov, Monthly Notices Royal Astron. Soc. **270**, 721 (1994).

[16] S. Koide, K.-I. Nishikawa and R.L. Mutel, Astrophys. J. **463**, L71 (1996).

[17] S. Koide, J.I. Sakai, K.-I. Nishikawa and R.L. Mutel, Astrophys. J. **464**, 724 (1996).

[18] S. Koide, Astrophys. J. **478**, 66 (1997).

[19] S. Koide, K. Shibata and T. Kudoh, Astrophys. J. **495**, L63 (1998).